

Fluctuation Mediated Interaction and Phase Separation of Nanoparticles in a Liquid Crystal Solvent

T. Bellini,^{1,2} M. Caggioni,¹ N. A. Clark,² F. Mantegazza,³ A. Maritan,⁴ and A. Pelizzola⁵

¹*INFN, Dipartimento di Chimica, Biochimica e Biotecnologie per la Medicina, Università di Milano, 20122 Milano, Italy*

²*Department of Physics and Ferroelectric Material Research Center, University of Colorado, Boulder, Colorado 80309, USA*

³*INFN, Dipartimento di Medicina Sperimentale, Università di Milano-Bicocca, 20126 Milano, Italy*

⁴*International School for Advanced Studies, INFN and ICTP, 34014 Trieste, Italy*

⁵*INFN, Dipartimento di Fisica, Politecnico di Torino, 10129 Torino, Italy*

(Received 17 March 2003; published 22 August 2003; corrected 16 September 2003)

Water-in-oil microemulsions of nanodroplets in the isotropic phase of a thermotropic liquid crystal exhibit, with decreasing temperature and in anticipation of a demixing transition, enhanced correlation in fluctuations of both molecular orientation and droplet concentration. Mean field modeling of this pretransition behavior, on the basis of a lattice in which the nanodroplets are introduced as holes, shows that the observed interdroplet attractive interaction is produced by the disordering effect of the droplets on the liquid crystal and mediated solely by paranematic fluctuations.

DOI: 10.1103/PhysRevLett.91.085704

PACS numbers: 64.70.Md, 61.30.St

In recent years the spatial organization of particles by anisotropic ordering in the suspending solvent has been pursued as a potentially exciting pathway to novel soft matter [1,2]. In this vein, Yamamoto and Tanaka reported the “transparent nematic” phase in a composite nematic liquid crystal (pentyl-cyanobiphenyl, 5CB), double tailed ionic surfactant (didodecyldimethylammonium bromide, DDAB), and water system [3]. The surfactant, which tends to form interfaces concave toward the water at organic-water interfaces, forms a water-in-oil type microemulsion of inverse micelles in the 5CB host. Upon cooling, these mixtures were reported to exhibit two phase transitions: first to a new optically isotropic transparent nematic phase and then to the coexistence of bulklike nematic (N) and surfactant-rich isotropic (I) phases. According to the interpretation, the new phase is actually a nematic phase in which elasticity and radial boundary conditions on the micelle surface combine to produce a nematic structure where the director is distorted on the 10 nm length scale.

In this Letter we present an experimental and theoretical study of the isotropic phase of the 5CB/DDAB/H₂O microemulsion (5DH μ em), which enables us to detect and characterize the pretransitional behavior anticipating the demixing transition. We find clear indication of the existence, in the I phase, of intermicellar attraction mediated by paranematic fluctuations. This is the first time that fluctuation-driven interactions are observed in the I phase of a liquid crystal (LC) composite system. In this Letter we offer evidence supporting a description of the 5DH μ em radically different from that previously proposed. Our data can be understood picturing the micelles as holes with free or semifree boundary conditions, whose dominant effect is to dilute the nematic order, thus becoming less soluble as the local nematic order is enhanced with decreasing T . We show that the notion of fixed boundary conditions on the droplet surfaces, which

has been demonstrated in emulsions of μ m dimension objects, is not applicable for nm scale micelles.

Microemulsions were prepared by diluting in 5CB a variable volume fraction ϕ of a well homogenized mixture of DDAB and water with weight ratio $c(\text{DDAB})/c(\text{H}_2\text{O}) = 9$. Before any measurement was taken, samples were kept at $T > 60^\circ\text{C}$ and stirred to ensure homogeneity. The system behavior was found to be very sensitive to the concentration of water and thus reliable sample preparation required careful control of evaporation and hydration of components and containers. We performed systematic observation of the phase transition occurring while lowering T at various initial values of ϕ , and measurement of the volumes of the coexisting phases resulting from gravitation induced macroscopic separation of a low density phase (isotropic and micelle rich) from a high density one (birefringent and micelle poor). The resulting micelle-LC consolution curve is shown in Fig. 1. The topology of the phase diagram is not new, and agrees with previous observation of dispersions of polymers and colloidal particles in LC [2,4,5] and with the prediction of models describing mixtures of rods and spheres [6,7].

Crucial information on the 5DH μ em system can be obtained by studying the pretransitional behavior in the isotropic phase while decreasing T toward the demixing transition. The basic characterization tool employed in this study was static and dynamic, polarized (VV) and depolarized (VH) light scattering at fixed wave vector ($q = 22 \mu\text{m}^{-1}$). As shown in Fig. 2(a), analysis of the intensity autocorrelation function $g(\tau) = \langle I(t + \tau)I(t) - I(t)^2 \rangle / \langle I(t)^2 \rangle$ for polarized and depolarized LS enables separation of the total scattered intensity (I_T) into contributions due to pretransitional paranematic fluctuations (I_{PN}) and a contribution due to scattering by the micelles (I_M). While paranematic orientational fluctuations (of characteristic time τ_{PN}) can be detected in the ns regime

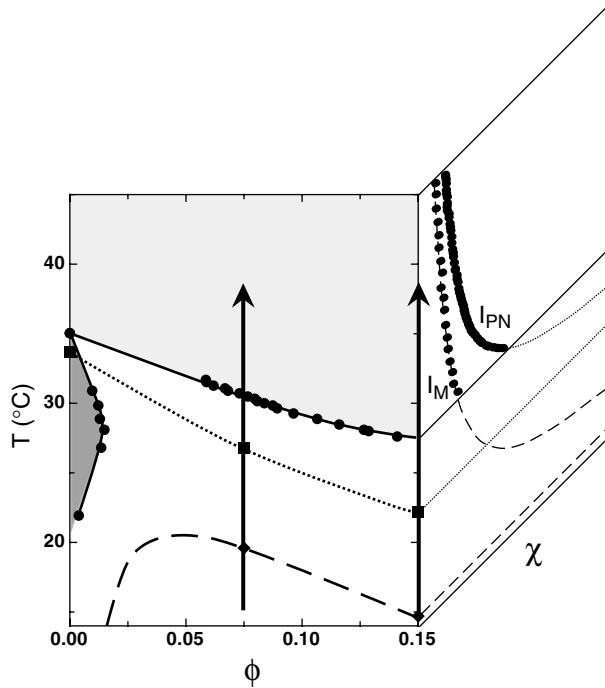


FIG. 1. Experimentally determined phase diagram of 5DH μ em as a function of temperature (T) and micellar concentration (ϕ). Continuous lines indicate the phase boundaries of the isotropic phase (light grey) and of nematic phase (dark grey) enclosing the (white) demixing region. Experiments performed at $\phi = 0.15$ and $\phi = 0.075$ (along the vertical arrows) enable determining the divergence T for the fluctuation in nematic order [squares, connected through the dotted line $T^*(\phi)$] and for the micellar osmotic compressibility [diamonds, laying on the spinodal dashed curve $T_M^*(\phi)$]. The meaning of T^* and T_M^* is sketched in the isometric projection plane on the right, where the behavior of the relevant susceptibilities (χ , from Figs. 2 and 3) is shown.

for both polarizations, long time collective micellar diffusion (of characteristic time τ_M) appears in $g(\tau)$ as a monoexponential relaxation in the μ s regime only when polarized light is collected [Fig. 2(a)], i.e., $(I_M)_{\text{VH}} = 0$. To make the contrast in $g(\tau)$ large and stable, and thus enable an accurate determination of I_{PN} and I_M , we have collected the scattered light with a single mode optical fiber. The T dependence of $I_{\text{VH}} \propto I_{\text{PN}}$ is shown in Fig. 2(b) for the case of bulk 5CB (crosses), as well as for 5DH μ em with $\phi = 0.075$ (full dots) and $\phi = 0.15$ (empty dots). $I_{\text{VH}}(T)$, which contains no direct contributions from micelles, exhibits classic isotropic-nematic mean field behavior, diverging as $1/(T - T^*)$ [8,9], to a ϕ dependent T^* (vertical lines in Fig. 2, and dotted line in the phase diagram, Fig. 1). In Fig. 2(c) we show $\tau_{\text{PN}}(\phi, T)$, as determined from $g(\tau)$, divided by $\eta(T)$, the viscosity of 5CB in the isotropic phase [10] extrapolated below the bulk T_{NI} according to its Arrhenius T dependence. The dynamics of 5DH μ em is also well described by I-N mean field behavior, $\tau_{\text{PN}} \sim \eta/(T - T^*)$ with the same $T^*(\phi)$

obtained from I_{VH} . Thus the effects of annealed disorder on both the static and dynamics of the orientational correlations in the isotropic phase of 5DH μ em are embodied in a simple depression of T^* with respect to 5CB (with maybe the exception of the dynamic data closest to T_{DM}), as illustrated clearly by the collapse on a single curve of τ_{PN}/η vs I_{VH} measured at various ϕ [Fig. 2(d)].

The bulk isotropic phase terminates at the first order NI transition $T_{\text{NI}} = 34.7^\circ\text{C} > T^*(\phi = 0) = 33.7^\circ\text{C}$. The 5DH μ em isotropic phase terminates at $T_{\text{DM}}(\phi) > T^*(\phi)$, when macroscopic phase separation takes place. The reduction of $I_{\text{PN}}(T)$ observed as ϕ is increased indicates that paranematic fluctuations are made increasingly unfavorable by the presence of the micelles. Conversely, intermicellar interactions are induced by paranematic fluctuations. Indeed, accompanying the

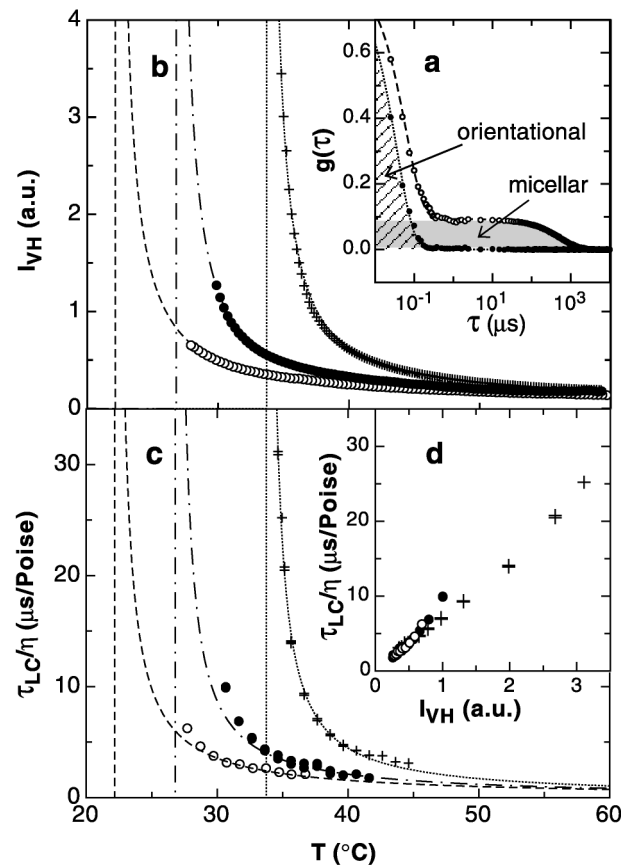


FIG. 2. (a) Intensity autocorrelation function $g(\tau)$ vs retardation time τ for polarized (open dots) and depolarized (full dots) scattered light. Shadows highlight the two different components. (b) Depolarized scattered intensity I_{VH} vs T for bulk 5CB (crosses), 5DH μ em with $\phi = 0.075$ (full dots) and with $\phi = 0.15$ (empty dots). Lines indicate $1/[T - T^*(\phi)]$ fitting curves, diverging at the T^* marked by the vertical lines. (c) Correlation time for paranematic fluctuations $\tau_{\text{LC}}(T)$ scaled with viscosity $\eta(T)$ and fitted to $1/[T - T^*(\phi)]$. Symbols as in (b). (d) Comparison of static (I_{VH}) and dynamic (τ_{LC}/η) behavior showing collapse of the 5DH μ em data on bulk.

growth in the correlation range for paranematic fluctuations is a growth in I_M , shown in Fig. 3, that cannot be explained in terms of the formation of a LC radial wetting layer of molecular thickness, which would bear a negligible optical contrast with the solvent and hence negligible enhancement of light scattering. The behavior of $I_M(T)$, proportional to ϕ only at high T (after the necessary hard sphere correction), reflects the presence of increasing fluctuations in micellar density as T decreases. Upon reducing T , I_M grows, indicating a growing osmotic compressibility of the micellar system, and thus a decreasing negative second virial coefficient. And hence the presence of attractive intermicellar interactions growing with decreasing T . Moreover, analysis of Fig. 3 in terms of virial expansion indicates stronger interactions for smaller ϕ , i.e., when the paranematic fluctuations are wider. The pretransitional growth of $I_M(T)$ is well described by a mean fieldlike behavior $(T - T_M^*)^{-1}$ (lines in Fig. 3) diverging to a temperature $T_M^* < T_{DM}$ (vertical lines). $T_M^*(\phi)$ locates the spinodal line. We find that T_M^* decreases with increasing ϕ for $\phi > 0.075$. However, for small experimentally inaccessible ϕ , T_M^* must take a positive slope since the system of highly diluted micelles necessarily approaches gaslike noninteracting behavior ($T_M^* \propto \phi$).

Further evidence of attractive interactions is provided by the slowing down of the micellar diffusion (inset of Fig. 3). The micellar hydrodynamic radius R extracted from $g(\tau)$ at high $T \approx 60^\circ\text{C}$ is $R \approx 20 \text{ \AA}$. Given the composition of the 5DH μ em, the average radius of the polar-apolar interface of the DDAB inversed micelles is

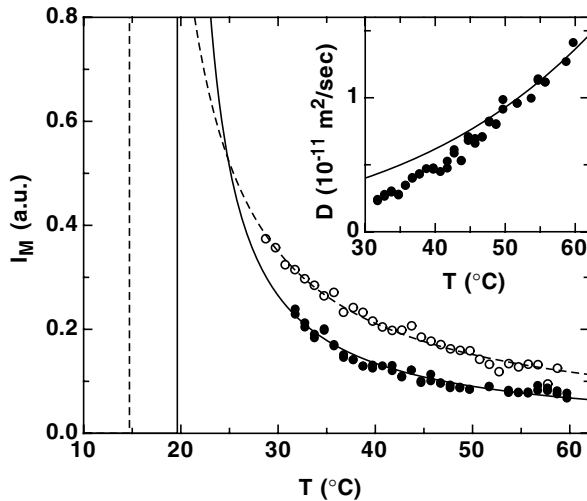


FIG. 3. Static (main figure) and dynamic (inset) behavior of the light scattered by the 5DH μ em droplets for $\phi = 0.075$ (full dots) and $\phi = 0.15$ (empty dots). The micellar osmotic compressibility (proportional to I_M) vs T has been fitted to $1/[T - T_M^*(\phi)]$ and diverge where marked by the vertical lines. Inset: micellar collective diffusion coefficient D vs T (dots) for $\phi = 0.075$; the line indicates the expected behavior of $D_{HS}(T)$ for hard spheres suspended in 5CB having $R = 20 \text{ \AA}$.

estimated in $R_l \approx 9.4 \text{ \AA}$ [11]. The measured R should be compared with R_l incremented by the DDAB alkyl chain length, which ranges from about 5 \AA (all chains compacted around the polar-apolar interface) to 15 \AA (fully extended chains). Upon lowering T , the diffusion coefficient $D(T)$ deviates from $D_{HS}(T)$, the diffusion coefficient expected from $\eta(T)$ and by keeping fixed the micellar size. As visible in the figure, the slowing down is substantial, reaching a factor of about 2 for $T = T_{DM}$.

This evidence from fluctuations in molecular orientational order (Fig. 2) and in micellar concentration (Fig. 3) suggests that the expulsion of micelles by orientational ordering, explicitly manifested at low T in the macroscopic phase separation, is at the root of the whole phase behavior of 5DH μ em. Nematic correlations (of size ξ_N , the nematic correlation length) appear more easily where the local micelle concentration is lower, and in turn force out micelles, thus further reducing the local amount of annealed disorder and increasing the local T^* , with the consequent increase of local nematic order. Thus the effective micellar attraction arises from repulsion of micelles by nematic fluctuations in a way more similar to the behavior of small molecular impurities in a nematic [12] than to that of macroscopic particles [13]. This notion is corroborated by the experimental coincidence between the average intermicellar distance d and the maximum value of $\xi_{N,\max} = \xi_0 [T^*/(T_{DM} - T^*)]^{1/2}$, with $\xi_0 \sim 10 \text{ \AA}$ [14]: for $\phi = 0.075$, $\xi_{N,\max} \approx 95 \text{ \AA}$, $d \approx 85 \text{ \AA}$; for $\phi = 0.15$, $\xi_{N,\max} \approx 75 \text{ \AA}$, $d \approx 70 \text{ \AA}$.

The phase behavior and divergent susceptibilities reported here can be described surprisingly well by a simple model system obtained by dilution of the classic Lebwohl-Lasher spin lattice model for NI transition [15]. In such a model either the sites of a cubic 3D lattice can host a headless unit vector \mathbf{s} free to rotate in the whole solid angle or they may be empty. The corresponding Hamiltonian is

$$H = -J \sum_{i,j} P_2(\mathbf{s}_i \cdot \mathbf{s}_j) \sigma_i \sigma_j - \mu \sum_i \sigma_i, \quad (1)$$

where $\sigma_k = 0, 1$ gives the site occupancy ($\sigma = 0$: empty site; $\sigma = 1$: occupied site), and μ is a chemical potential controlling the concentration of empty sites. In this model there is no anchoring of LC molecules at the micelle surface, in agreement with the notion that the extrapolation length even for strong anchoring is much larger than the size of the nanodroplets. The model Eq. (1) was first proposed to describe the phase behavior of mixtures of rods and spheres [6] and later reconsidered to study the isotropic-nematic-vapor phase coexistence [7]. Given the experimental evidence on the pretransitional behavior, we have reconsidered the model in Eq. (1) in mean field approximation, and calculated the phase diagram complete with the susceptibilities, not available from previous studies. Namely we extracted the spinodal ($T_M^*(\phi)$) and the nematic divergence ($T^*(\phi)$) lines, as shown in Fig. 4.

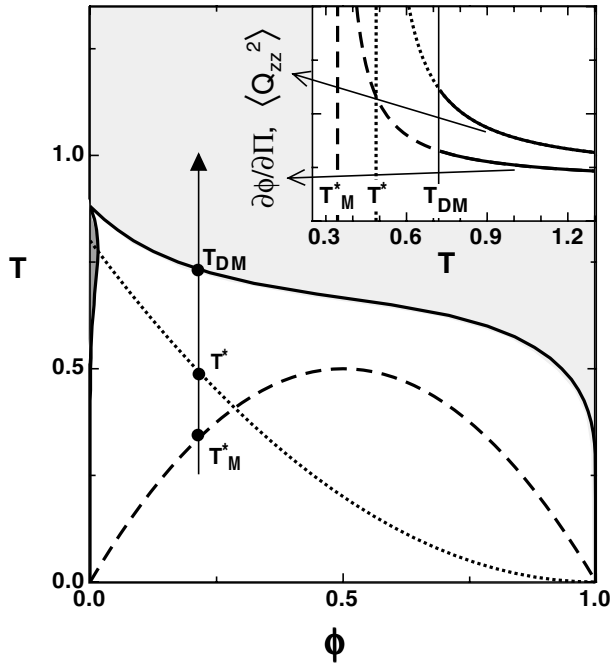


FIG. 4. Phase diagram obtained from the mean field analysis of the diluted Lebwohl-Lasher model in Eq. (1). Continuous lines indicate the phase boundaries of the isotropic (light grey) and nematic (dark grey) phases enclosing the (white) demixing region. The dashed line is the spinodal curve $T_M^*(\phi)$, where the micellar osmotic compressibility $\partial\phi/\partial\Pi$ diverges. The dotted line is the divergence temperature $T^*(\phi)$ for the nematic correlation length and for the mean square amplitude of nematic order fluctuations ($\langle Q_{zz}^2 \rangle$). The predicted divergence of two such susceptibilities along the line indicated by the arrow is plotted in the inset.

In the inset we show the predicted behavior of the two relevant susceptibilities: the micellar osmotic compressibility $\partial\phi/\partial\Pi$ and the mean squared amplitude of the nematic order parameter ($\langle Q_{zz}^2 \rangle$), to be compared with $I_M(T)$ and $I_{VH}(T)$, respectively, display $(T - T_M^*)^{-1}$ and $(T - T^*)^{-1}$ divergence characteristics of mean field behavior. The $T_{DM} - T^*$ gap for the pure nematic as well as the ϕ corresponding to the maximum in the spinodal curve are both much larger than the corresponding observed quantities. These expected shortcomings are consequences, respectively, of the intrinsic limitations of the mean field approximation and of having assumed that micelles and LC molecules have equal volumes [16].

As it appears by comparing Fig. 4 with the experimental results, the model succeeds in characterizing all the observed phenomena, thus revealing that the $5DH\mu\text{em}$ behavior is in the largest part a consequence of the dilution effect that the nanoinclusions have on the LC. The simplicity of the proposed model, in which there is no explicit interaction between micelles, strengthens the evidence that increased micellar osmotic compressibility,

and thus effective attractive interactions, result simply as a consequence of the fluctuations of the liquid crystal degrees of freedom. The rationale of such a fluctuation-driven interaction is offered by theoretical considerations, which indicate that sufficiently small impurities incorporated in the nematic phase display long ranged attraction due to orientational fluctuations of the LC [17]. This is because impurities depress the local nematic order, and are thus segregated to minimize the total free energy. We argue that the same mechanism should be present in the I phase but with an exponential cutoff at the correlation length of liquid crystal fluctuations. This behavior is reminiscent of the Casimir forces, expected between generic quenched objects (not annealed like in the case of our micelles) immersed in a fluctuating fluid [18].

The agreement of data and theory offers unambiguous understanding of the equilibrium properties of this composite system, enlightening the profound difference in the behavior of LC suspensions of nano and microparticles.

This work was supported by NATO (Collaborative Linkage Grant), NSF (DMR-0072989 and MRSEC DMR-0213918) and NASA (NAG 8-1665).

- [1] P. Poulin, H. Stark, T. Lubensky, and D. Weitz, *Science* **275**, 1770 (1997).
- [2] J.-C. Loudet, P. Barois, and P. Poulin, *Nature (London)* **407**, 611 (2000).
- [3] J. Yamamoto and H. Tanaka, *Nature (London)* **409**, 321 (2001).
- [4] C. Shen and T. Kyu, *J. Chem. Phys.* **102**, 556 (1995).
- [5] V. Anderson, E. Terentjev, S. Meeker, J. Crain, and W. Poon, *Eur. Phys. J. E* **4**, 11 (2001).
- [6] R. Hashim, G.R. Luckhurst, and S. Romano, *Proc. R. Soc. London, Ser. A* **429**, 323 (1990).
- [7] M. Bates, *Phys. Rev. E* **64**, 051702 (2001).
- [8] T. Stinson and J. Litster, *Phys. Rev. Lett.* **25**, 503 (1970).
- [9] P.-G. de Gennes, *Mol. Cryst. Liq. Cryst.* **12**, 193 (1971).
- [10] J. Constant and E. P. Raynes, *Mol. Cryst. Liq. Cryst.* **62**, 115 (1980).
- [11] M. Monduzzi, F. Caboi, F. Larché, and U. Olsson, *Langmuir* **13**, 2184 (1997).
- [12] T. D. Gierke and W. H. Flygare, *J. Chem. Phys.* **61**, 2231 (1974).
- [13] A. Borstnik, H. Stark, and S. Zumer, *Phys. Rev. E* **60**, 4210 (1999).
- [14] P.-G. de Gennes and J. Prost, *The Physics of Liquid Crystals* (Clarendon, Oxford, 1993), 2nd ed.
- [15] P. Lebwohl and G. Lasher, *Phys. Rev. A* **6**, 426 (1972).
- [16] D. Blankschtein, G.M. Thurston, and G.B. Benedek, *Phys. Rev. Lett.* **54**, 955 (1985).
- [17] D. Bartolo, D. Long, and J.-B. Fournier, *Europhys. Lett.* **49**, 729 (2000).
- [18] H. Li and M. Kardar, *Phys. Rev. A* **46**, 6490 (1992).